Parallel Plate Capacitive MEMS Mirror

Mirza Muhammed Karlidağ
Electrical and Electronics Engineering Department
Koç University
Ankara, Turkey
mkarlidag15@ku.edu.tr

Deniz Karadayı
Electrical and Electronics Engineering Department
Koç University
Istanbul, Turkey
dkaradayi16@ku.edu.tr

***Abstract*—In this report, we aim to explain the details and specifications of our design for a parallel plate MEMS capacitor which will be used to control a movable mirror in an interferometer device. We made experimental calculations to optimize a system reaching a maximum steady displacement with minimum input voltage. Our report includes design specifications, sketches and simulation results obtained from MATLAB and CAD tool of such a device.**

Keywords—Parallel Plate MEMS Capacitor, ES Actuator, Michelson Interferometer, MATLAB, Pull-in Effect

I. INTRODUCTION

A parallel plate MEMS is a MEMS device where two parallel plates are used to create a capacitor that is driven by a voltage to build an actuator. It can be used for various applications. Here, we use it to move a mirror which is a part of an interferometer system. The device can be used to measure the wavelength of light.

A. Michelson Interferometer

Michelsen Interferometer is a specific type of interferometer that uses a beam splitter and a movable mirror to measure small displacements or wavelengths as shown in [Fig. 1, 1]. The light beam from the light source is split into two light beams that travel through two perpendicular paths which end up with separate mirrors one of which is movable. Then, reflected light beams come to the beam splitter and are directed to a photodetector or a plane by the beam splitter. Here, interference of light occurs where light beams coming from two mirrors constructively and destructively interfere. The observed interference pattern depends on the phase of the light beam reflected from the movable mirror. As the mirror moves, the interference pattern changes as seen from [Fig. 2, 2] and [Fig. 3, 2].

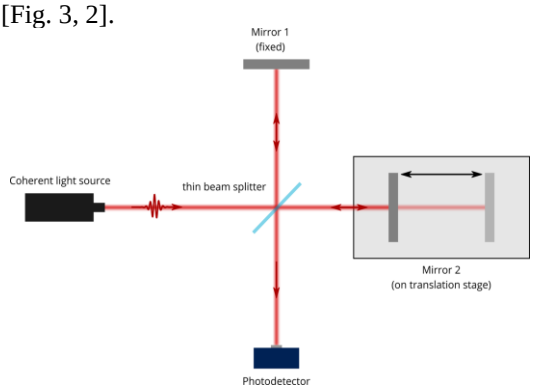

Fig. 1 – Michelson Interferometer

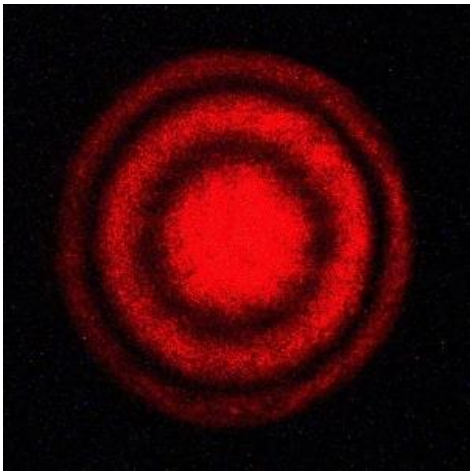

Fig. 2 – Constructive Interference

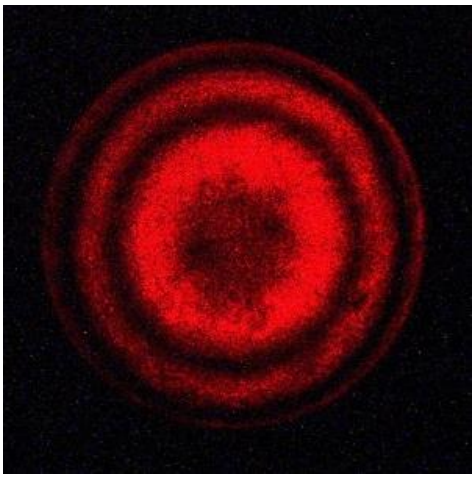

Fig. 3 – Destructive Interference

Assuming the mirrors were equidistant from the splitter at first, we could observe a constructive interference at the center of the interference pattern. If the mirror moved by $\lambda/4$, the phase of the light reflected from the movable mirror is shifted by π which causes destructive interference at the center of the pattern. If the mirror moved $\lambda/2$, the phase is shifted by 2π which again causes constructive interference. This process is shown and explained in [Fig. 4, 3]. By counting the number of interference fringes as the mirror moves, one can calculate the displacement by the formula $\Delta d = m\,\lambda/2$ where m is the number of fringes, λ is the wavelength of the light beam and Δd is the displacement.

Knowing displacement, one can calculate wavelength as well.

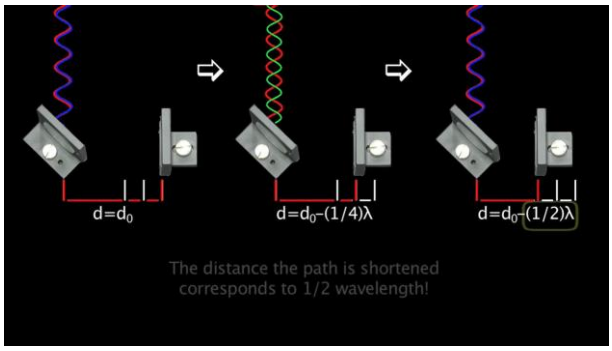

Fig. 4 – Effect of Movable Mirror on Interference

II. Theory, Design Concept

Our design for the project is shown in Fig. 5 which is created using a 2D design and drafting software called QCAD. Two parallel plates form a capacitor and with a spring and a damper connected to it, the whole system can be represented with a spring-mass-damper mechanical system whose electrical equivalent is shown in [Fig. 6, 4]. The displacement of the movable plate is a function of the input voltage. The applied voltage leads to an electrostatic force between plates (F_{es}), and the occurred displacement also generates a resistive force (F_{mech}) in the opposite direction due to the mechanical load between the movable plate and fixed point. For appropriate voltage configurations and parameters, these forces cause the left plate to move as a result causing Mirror 2 to move as well.

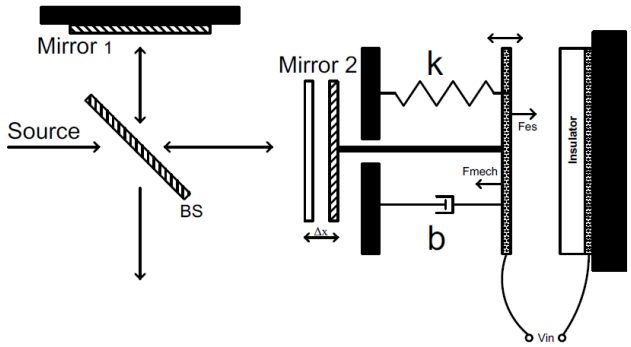

Fig. 5 – Parallel Plate MEMS Capacitor Design

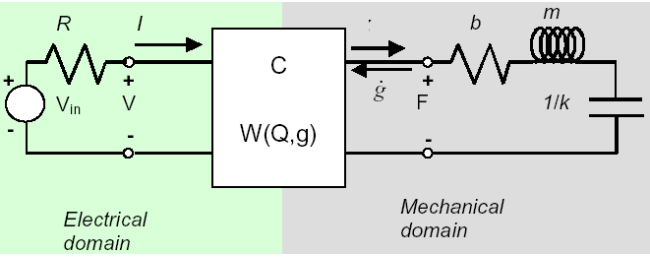

Fig. 6 – Electrical Equivalent of the system

[Fig. 6] also represents a transducer which is a device that converts energy from one form to another. Here, it converts mechanical energy to electrical energy. The dynamics of this electromechanical system specifies the displacement behavior of the movable plate. Related formulations about the system are given below according to the parameters shown in [Fig. 6].

$$I = \dot{Q} = \frac{1}{R}\left(\frac{Qg}{A\varepsilon}\right) \quad \text{Eq. 1}$$

$$F = \frac{Q^2}{2A\varepsilon} = -b\dot{g} - m\ddot{g} - k(g - g_0) => \quad \text{Eq. 2}$$

$$m\ddot{g} + b\dot{g} + k(g - g_0) + \frac{Q^2}{2A\varepsilon} \quad \text{Eq. 3}$$

$$x = \begin{bmatrix} x_1 \\ x_2 \\ x_3 \end{bmatrix} = \begin{bmatrix} Q \\ g \\ \dot{g} \end{bmatrix} \quad \text{Eq. 4}$$

$$\dot{x} = \begin{bmatrix} \dot{x}_1 \\ \dot{x}_2 \\ \dot{x}_3 \end{bmatrix} = \begin{bmatrix} Q \\ g \\ \dot{g} \end{bmatrix} = \begin{bmatrix} \frac{1}{R}\left(V_{in} - \frac{x_1 x_2}{A\varepsilon}\right) \\ x_3 \\ -\frac{1}{m}\left(bx_2 + k(x_x - g_0) + \frac{{x_1}^2}{2A\varepsilon}\right) \end{bmatrix} \quad \text{Eq. 5}$$

Eq. 1 shows the relations between the charge and the current which is useful to relate voltage and capacitance. Eq. 2 is a second-order ODE which is the characteristic equation of s mass-spring-damper system. The whole mechanical system is replaced with its electrical equivalent. If we assign the variables on the right-hand side of the equation to the left-hand side, we get Eq. 3. By assigning appropriate variables to a 1x3 matrix "x" in Eq. 4, we can calculate, Q, $\dot{g}$, and $\ddot{g}$ using matrix manipulations. By successfully calculating variables, we get Eq. 6.

$$s^2 + 2\alpha s + {\omega_0}^2 = 0 \quad \text{Eq. 6}$$

Here, ω_0 is the natural frequency (undamped resonant frequency) which is the oscillation frequency caused by F_{es} and F_{mech}, and $\frac{\omega_0}{2\alpha}$ is the quality factor (Q-factor).

III. Theory and Working Principle

As explained in the previous section, a parallel plate ES actuator is used to control a movable mirror that is a part of an interferometer system. As the voltage is applied to the device, displacement occurs, and we can calculate the displacement with the equations stated above (Eq. 5). Using such a device, we can calculate the wavelength of a light beam with the equation $\lambda = 2\Delta d/m$ as stated in the first section.

IV. Pull-In Effect

The Pull-in effect is an important phenomenon in ES actuator design. In the static equilibrium condition, the electrostatic force between plates and the mechanical force of the dynamic part of the system are equal and constitute stability. If the electrostatic force is increased by the voltage at this point, mechanical force becomes unable to resist the ES force, and the system shifts to an unstable fall which possibly ends up colliding between the plates, at the same time, shortcut in the electrical system. To prevent this collision, we place an insulator between plates to provide a minimum gap between two plates no matter what the input voltage is. The limiting voltage which the instability begins just after crossing it is called pull-in voltage. The behavior of

such pull-in phenomena is shown in [Fig. 7, 4]. Here, voltage increases in the direction of the right arrow that is showing up and decreases in the direction of the other arrow. As explained above, increasing voltage cause an unstable state and ends up in the collision of plates. This situation is called the pull-in effect and the distance and voltage which this happens are called pull-in distance and pull-in voltage, respectively. After that point, decreasing the voltage to pull-in voltage again is not going to do any change since plates are now stuck together with an insulator separating them. Thus, it is harder to separate them and bring the system to its initial position. This also can be observed in the [Fig. 7] as well. The voltage to separate plates is smaller than the pull-in voltage.

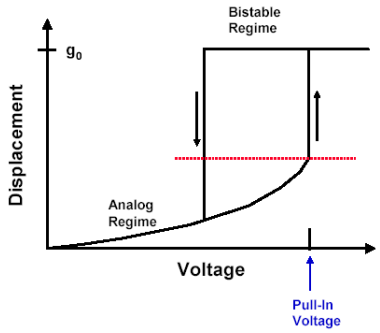

Fig. 7 – Behavior of Pull-in Effect

V. Notes on Nemirovsky's Foundations

According to Nemirovsky et al., the total energy (sum of mechanical and electrical energy) of an electrostatic actuator is shown below in [Fig. 8, 5]. In the graph, minimums show stable equilibrium points while maximums represent unstable equilibrium points. As the charge between plates is increased, these two states come closer to a critical point where the first and second derivatives of the energy with respect to the mechanical displacement become zero [5].

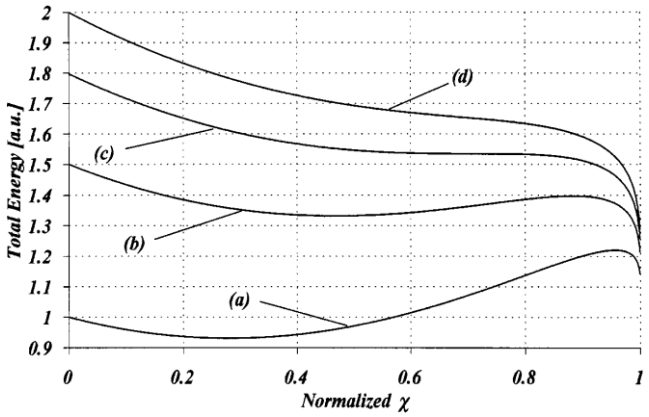

Fig. 8 – Total Energy vs. Displacement Graph of ES Actuator

Total Energy U_T is the sum of electrostatic energy U_E and mechanical energy U_M in the ES actuator such as the following.

$$U_T = U_M + U_E = U_M + \frac{CV^2}{2} \qquad \text{Eq. 7 [5]}$$

Since this equation is a function of displacement, and the electrostatic and the mechanical forces act against each other, the formula evolved as follows.

$$U_T(\chi) = \frac{1}{2}V^2C(\chi) - U_M(\chi) \qquad \text{Eq. 8 [5]}$$

For critical stability, two energy-related conditions should be satisfied, and the first and second derivative of the total energy with respect to displacement must be equal to zero.

$$\frac{\partial U_T}{\partial \chi} = 0, \frac{\partial^2 U_T}{\partial \chi^2} = 0 \qquad \text{Eq. 9 [5]}$$

From their calculations, Nemirovsky et al., provide a formula for V_{PI} which is pull-in voltage as shown below.

$$V_{PI} = \sqrt{2\frac{\partial U_M(\chi_{PI})}{\partial \chi} \Big/ \frac{\partial C(\chi_{PI})}{\partial \chi}} \qquad \text{Eq. 10 [5]}$$

VI. Fabrication

Miller et al. explained the details and fabrication process of an ES actuated MEMS mirror in their paper. Considering the similarity between their research and our project, it would be a good idea to adapt their fabrication processes for our design.

Miller et al., first start with the mirror which they produced by depositing "low stress silicon nitride by low-pressure chemical vapor deposition onto both sides of a double side polished <100> silicon wafer." [6]. Then, the wafer is patterned with photoresist on the front, and the backside is patterned with a mask. After that, nitride is removed from the exposed areas by a plasma dry-etch. Then, the wafer is placed in a bath of potassium hydroxide with isopropanol. Eventually, both sides are coated with gold.

VII. Simulation Results

A. Design Specifications

Design Parameters		Dependent Parameters	
initial gap	300 µm	mass of plate	582.5 ng
minimum gap	60 µm	mass of mirror	27 ng
width of plate	50 mm	damping coefficient (α)	785.40
length of plate	50 m	spring coefficient (k)	0.241 N/m^2
thickness of plate	0.1 µm	damper coefficient (b)	9.57 * 10^{-4}
resonant frequency	100 Hz	natural resonant frequency (w0)	628.32 rad/s
Q factor	0.4		
density of plate (Si)	2330 g/m^3		
width of mirror	1 mm		
length of mirror	1 mm		
thickness of mirror	0.1 µm		
density of mirror (Al)	2700 g/m^3		

Table I – Chosen Design Parameters of the System, and Dependent Parameters

The specification that we used in our system in given in the previous table. We arranged these parameters to have the maximum possible displacement while minimizing the input voltage. By using these parameters, the result of our MATLAB simulation displaying the DC voltage and displacement can be shown in Fig. 9.

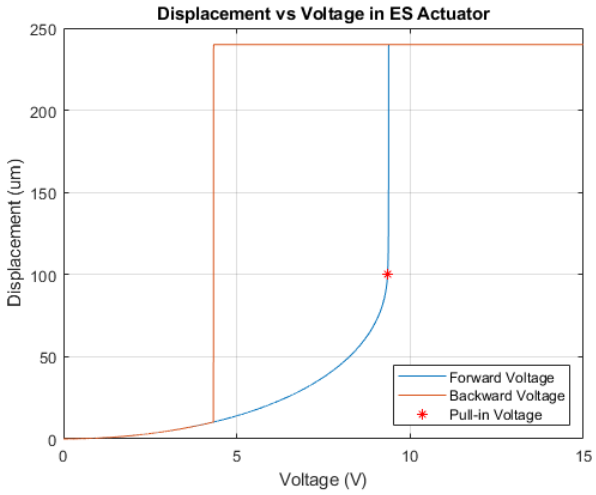

Fig. 9 – Displacement vs Voltage, Voltage first increasing up to 15 V, and decreasing back.

As it can be seen in the graph, the systems shows a pull-in behavior at V = 9.34 V, corresponding a pull-in displacement 99.9 µm. Which is approximately the one third of the initial gap. Here, we can deduce that, it is not possible to exceed this ratio by using a voltage controlled electrostatic parallel plate actuator as it is supported by the Nemirovsky's article as well [5]. The system reaches to an unstable point after exceeding the pull-in voltage, so it is not possible to adjust a steady result for higher voltages. The following Fig. 10 shows the displacement behavior at different constant dc voltage application by time.

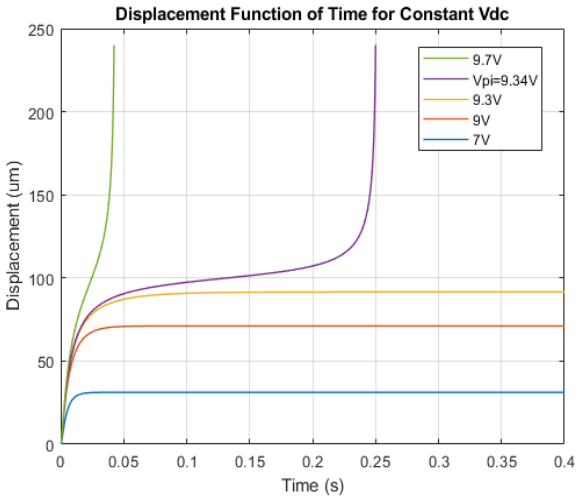

Fig.10 – Displacement Behavior for Different DC Voltages with respect to Time

This graph shows the settlement of displacement by time. Since the system is overdamped second order mechanical system, it reaches a steady equilibrium quickly. However, when the input voltages approach to Vpi, the system cannot find an equilibrium and dramatic jump in the displacement occurs. For, higher voltages than pull-in voltage, the system much quickly reach an instability.

To sum up, the reason why we chose these parameters depends on this phenomenon so that we can avoid the pull-in voltage while we are reaching a maximum displacement we can. Besides, maximize the pull-in voltage of system that we experience pull-in effect so that we can increase the displacement before pull-in occurs. Another criterion that we consider was to power consumption. In other words, we do not want to use absurd levels of voltages just to have a greater displacement, so we tried to find and optimal point. The following Table II explains the other specification we tried to observe the behavior of the system.

Changed Parameter	Vpi (V)	Xpi(µm)
0.5m (3.0475e-07)	6.6100	98.3646
1.3m (7.9235e-07)	10.6600	100.8466
2m (1.2190e-06)	13.2200	101.8200
Q = 0.5	9.3410	97.6247
Q = 1	9.3300	95.2003
Q = 5	8.8920	66.9341
f0 = 80 Hz	7.4880	103.0388
f0= 120 Hz	11.2100	98.5116

Table II – Results of Simulation with the Selection of Different Parameters (m refers to the total mass we eventually decided for our design)

From Table II, you can see that increase in mass also increases the required voltage to reach displacement while the maximum voltage does not increase remarkably. The increase in Q, which makes system more responsive to change and causes longer settling times, dramatically decreases the displacement which we, in fact, try to maximize. In addition, the increase in resonant frequency also increases the Vpi dramatically. The reason why we use 100 Hz instead of 80 Hz or lower is the default expectation for our design was the use of 100 Hz and initial gap 300 µm.

B. Effects of AC Voltage: Frequency Selection

Up to here, we displayed the results of DC voltage. Now, I would like to present the effect of AC voltage on the system. First of all, let us look at the frequency change of AC voltage. The following Fig. 11 represent the change in displacement in its steady state response for the application of AC voltages at different frequencies.

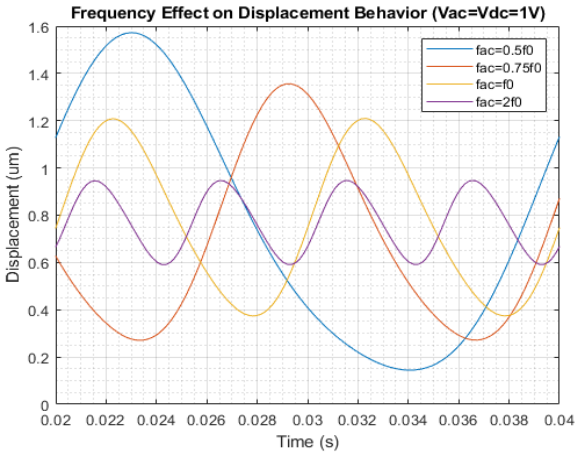

Fig.10 – Displacement Behavior for AC Voltages with Different Frequencies

It shows that the increase in the frequency of the AC voltage decreases the amplitude of the displacement oscillation so that the displacement is being pulled by the voltage before it reaches its maximum values for the higher frequencies. Therefore, it is much reasonable to choose the Vac frequency lower to have greater displacement freedom. The following Table III shows the corresponding center of Displacement and gain of oscillation respective to frequencies at Vac = Vdc = 1V. You can see that while center of displacement is steady the gain decreases.

Frequency	Center of Oscillation (μm)	Gain of Oscillation (μm)
50 Hz (0.5 $f_{resonant}$)	0.7706	0.8033
75 Hz (0.75 $f_{resonant}$)	0.7695	0.5872
100 Hz (1 $f_{resonant}$)	0.7737	0.4361
200 Hz (2 $f_{resonant}$)	0.7731	0.1741

Table III – Frequency vs Center and Gain of Oscillation

C. Effects of AC Voltage: DC and AC Components

The DC and AC components of the voltage both have an increasing effect on center and gain of oscillation. However, the dominances of their effects are varying. The following Fig. 11 and 12 shows the Vdc and Vac effect while the other component kept steady. The applied parameters are given in the tables following the figures.

Vac	**Vdc**	**Center of Oscillation (um)**	**Gain of Oscillation (um)**
1 V	2 V	2.3342	1.5373
1 V	4 V	8.9455	3.1964
2 V	4 V	9.8552	6.6878
4 V	4 V	13.9382	27.9018

Table III – Vac-Vdc vs Center and Gain of Oscillation

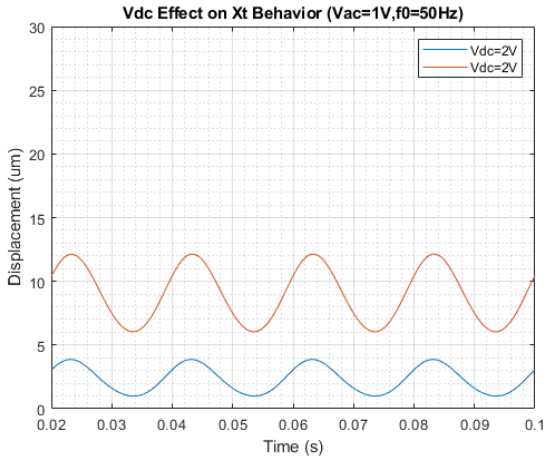

Fig.11 – Displacement Behavior for Different DC Voltage Components

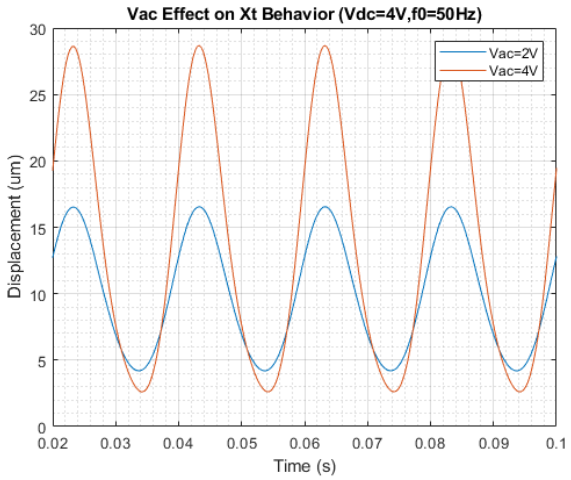

Fig.12 – Displacement Behavior for Different AC Voltage Components

Therefore, we can deduce that the DC has a greater effect on the change of the center of oscillation while AC has a greater effect on the change of the gain of oscillation. The following Fig. 13 and 14 explains better the effect of the change in AC and DC component to both of the variables of oscillation

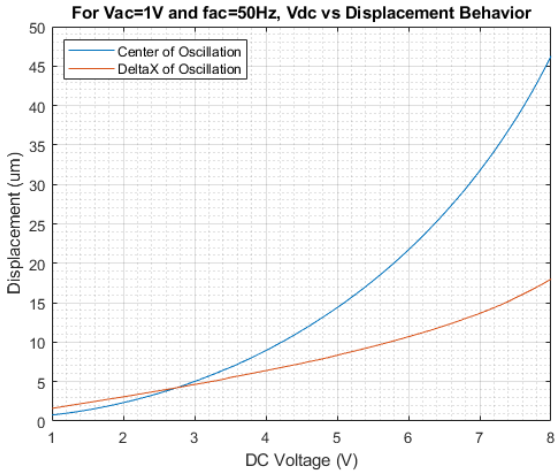

Fig.13 – Change of Center and Gain of Oscillation With Respect to Vdc

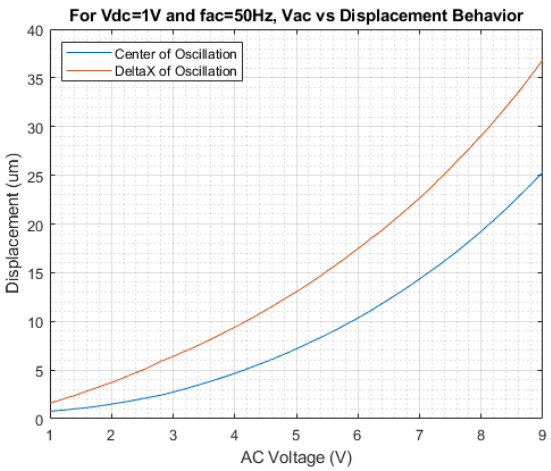

Fig.14 – Fig.13 – Change of Center and Gain of Oscillation With Respect to Vac

VIII. Conclusion

As a result, our design can displace up to 100 µm steadily so that it can measure the wavelength up to 200 µm. The desired adjustment can be done both by the use of DC and AC components. According to the adjustments in the voltage values, multiple types of displacement with multiple freedom options can be applied. The single use of DC voltage from 0 to 15 V gives you the ability of exact plate-positioning between 0 to 100 µm. In addition, including the AC voltage component to the equation, it is possible to obtain a steady displacement oscillation which can be adjust to the half of the beam's wavelength to measure. The relations we have explained and provide data about can help users to adjust their systems to meet their needs.

IX. References

[1] "The Michelson Interferometer - A Laser Lab Alignment Guide", WiredSense, 2021. [Online]. Available: https://www.wiredsense.com/tutorials/the-michelson-interferometer-a-laser-lab-alignment-guide. [Accessed: 17- Jan- 2021].

[2] "84.30 -- Michelson interferometer", Web.physics.ucsb.edu, 2021. [Online]. Available: http://web.physics.ucsb.edu/~lecturedemonstrations/Composer/Pages/84.30.html. [Accessed: 17- Jan- 2021].

[3] The Technical Services Group of MIT's Department of Physics. "Michelson Interferometer", YouTube, 22 June, 2012. [Video file]. Available: https://www.youtube.com/watch?v=j-u3IEgcTiQ. [Accessed: 17- Jan- 2021].

[4] H. Urey, Class Lecture, Topic: 'lec04_ESactuators', College of Engineering, Koç University, 2021.

[5] Y. Nemirovsky and O. Bochobza-Degani, " A methodology and model for the pull-in parameters of electrostatic actuators," in Journal of Microelectromechanical Systems, vol. 10,no. 4, pp. 601-615, Dec. 2001, doi: 10.1109/84.967384

[6] S. R. Bhalotra, J. D. Mansell, H. L. Kung and D. A. B. Miller, "Parallel-plate MEMS mirror design for large on-resonance displacement," 2000 IEEE/LEOS International Conference on Optical MEMS (Cat. No.00EX399), Kauai, HI, USA, 2000, pp. 93-94, doi: 10.1109/OMEMS.2000.879642.

[7] O. Degani et al., "Pull-in study of an electrostatic torsion microactuator," in Journal of Microelectromechanical Systems, vol. 7, no. 4, pp. 373-379, Dec. 1998, doi: 10.1109/84.735344.

[8] Elshenety, E. El-Kholy, A. Abdou, M. Soliman and M. Elhagry, "A flexible model for studying fringe field effect on parallel plate actuators", Journal of Electrical Systems and Information Technology, vol. 7, no. 1, 2020. Available: 10.1186/s43067-020-00022-7.a

[9] H. Urey, Class Lecture, Topic: 'lec06_dynamics', College of Engineering, Koç University, 2021.

[10] O. Manzardo, H. Herzig, C. Marxer and N. de Rooij, "Miniaturized time-scanning Fourier transform spectrometer based on silicon technology", Optics Letters, vol. 24, no. 23, p. 1705, 1999. Available: 10.1364/ol.24.00170